


Article

Seasonal Shifts in Cold Tolerance and the Composition of the Gut Microbiome of *Dendroctonus valens* LeConte Occur Concurrently

Zehai Hou, Yaxin Dong, Fengming Shi, Yabei Xu, Sixun Ge, Jing Tao, Lili Ren  and Shixiang Zong *

Key Laboratory of Beijing for the Control of Forest Pests, Beijing Forestry University, Beijing 100083, China; houzehai@bjfu.edu.cn (Z.H.); dongyaxindyx@163.com (Y.D.); shifengming@bjfu.edu.cn (F.S.); xuyabei@bjfu.edu.cn (Y.X.); gsx_pieris@163.com (S.G.); taojing1029@hotmail.com (J.T.); lily_ren@bjfu.edu.cn (L.R.)
* Correspondence: zongshixiang@bjfu.edu.cn



Citation: Hou, Z.; Dong, Y.; Shi, F.; Xu, Y.; Ge, S.; Tao, J.; Ren, L.; Zong, S. Seasonal Shifts in Cold Tolerance and the Composition of the Gut Microbiome of *Dendroctonus valens* LeConte Occur Concurrently. *Forests* **2021**, *12*, 888. <https://doi.org/10.3390/f12070888>

Academic Editors: Adrian Lukowski and Marian J. Giertych

Received: 14 May 2021

Accepted: 5 July 2021

Published: 7 July 2021

Publisher's Note: MDPI stays neutral with regard to jurisdictional claims in published maps and institutional affiliations.



Copyright: © 2021 by the authors. Licensee MDPI, Basel, Switzerland. This article is an open access article distributed under the terms and conditions of the Creative Commons Attribution (CC BY) license (<https://creativecommons.org/licenses/by/4.0/>).

Abstract: *Dendroctonus valens* LeConte, an invasive bark beetle, has caused severe damage in pine forests and has the potential to disperse into new geographic ranges in China. Although the gut microbiota of *D. valens* and its fundamental role in host fitness have been investigated widely, little is known about the relationship between the seasonal shifts of both cold tolerance and the gut microbiome of *D. valens* during overwintering, which occurs at the larval stage. In this study, to examine seasonal variations in the composition of the microbiome, we collected *D. valens* larvae in September (autumn), January (winter), and May (spring), and then analyzed the bacterial and fungal communities of the gut via sequencing of partial 16S rRNA and ITS genes. In addition, changes in the supercooling capacity and antioxidant enzyme activities of *D. valens* larvae collected in the different seasons were evaluated. Overwintering resulted in changes to microbial communities. In particular, the abundances of *Enterobacter*, *Serratia*, *Erwinia*, and *Klebsiella* decreased during overwintering. Concurrent with these changes, the cold tolerance of *D. valens* larvae was enhanced during overwintering, and the activities of the antioxidant enzymes catalase and peroxidase were reduced. We hypothesize that seasonal shifts in the gut microbiome may be connected to changes in cold tolerance and antioxidant enzyme activity in *D. valens*. It will be worthwhile to confirm whether seasonal changes in the microbiome contribute to the success of host overwintering.

Keywords: antioxidant enzyme; cold-hardiness; overwintering; red turpentine beetle; supercooling point; symbiosis

1. Introduction

Insects are chronically infected by microorganisms, most of which are beneficial or even obligatory to their insect hosts [1,2]. The large majority of these infecting microbes are colonized in the gut of their host, where they aid the digestion of unpalatable food components, improve undernourished diets, help their hosts defend against predators, parasites, and pathogens, and even affect host physiological action by neuroendocrine signaling [1–4]. Therefore, changes in the microbial community can affect a number of host phenotypes [2].

Insects in temperate regions are exposed to a prolonged cold during winter [5]; thus, their microbiomes are undergoing the same temperature changes. Overwintering insects undergo deep seasonal changes in feeding [6], intestinal contents [7], immune system [8], and physiological function [9]. These seasonal changes in host physiology have the potential to affect the composition of the gut microbiome [10]. For instance, Wang et al. [11] revealed that gut bacterial communities from Chinese white pine beetle *Dendroctonus armandi* Tsai and Li exhibited variation in relative abundance during overwintering stage. Ferguson et al. [12] demonstrated that seasonal changes in temperature shift the composition of the gut microbiome in the spring field cricket, *Gryllus veletis* (Alexander

and Bigelow), and this effect is accompanied by the changes in the physiology of *G. veletis*, which brings immunity and response to the cold. However, current knowledge of the seasonal shift of the insect gut microbiome under low temperatures and during overwintering is still insufficient [12].

The red turpentine beetle (RTB), *Dendroctonus valens* LeConte (Coleoptera: Curculionidae, Scolytinae), is found naturally throughout most regions of North and Central America. Specifically, its range extends from the Northwest Territories in Canada to Honduras, excluding south-eastern USA [13]. The RTB is commonly recognized as a secondary pest in its native range but has become an aggressive, univoltine, tree-killing species in China. Since it first appeared in Shanxi Province in the late 1990s, the RTB has caused the death of exceeding 10 million healthy pines in northern China [14,15]. In Shanxi Province, pupation of overwintered larvae begins in early June, and eclosion begins in early July [16]. Oviposition begins in middle July, and incubation of egg begins in last July. In September, RTBs overwinter as mature larvae, adults, even pupae, 2nd- or 3rd-instar larvae [16]. In recent years, alongside the distribution of pine forest, RTB has spread to more northern regions of China, such as Liaoning province and the Inner Mongolia Autonomous Region [17–19]. Due to the severity of the RTB outbreak in China, various aspects of the invasion dynamics of this insect have been studied [14], including its ecology [20] and yeast associates [15], the bioactivities of microorganisms against host defensive monoterpenes [21], the survival of RTB and its adaptability to a climate warming scenario [22], and the diversity of fungi associated with the insect [23–25].

Freezing-intolerant insects are unable to survive internal ice formation [26,27]; however, many of overwintering insects can avoid the lethal effects of tissue freezing by enhancing the supercooling capacity of their body fluids, a process that is achieved by the accumulation of low molecular-weight polyols and sugars and the elimination of some ice nucleators in the gut [28]. In our previous study, we found that glycerol, trehalose, and sorbitol may help RTB larvae to survive during overwintering [29]. Recently, Zhao et al. [19] compared the transcriptomes of wintering and non-wintering adult and larval *D. valens*, then identified a series of genes associated with cold tolerance. Another factor limiting the supercooling ability of insects is the existing of nucleating agents catalyzing ice formation at high subzero temperatures [30]. A large number of studies have demonstrated that ice nucleating active (INA) microorganisms in the insect gut regulate the SCP of their host [28]. For example, the fire-colored beetle, *Dendroides canadensis* Latreille, actively regulates its gut microbiome to avoid freezing during the winter, by suppressing bacteria that lead to ice nucleation [7]. An INA fungus, *Fusarium* sp. was isolated from the gut of larvae of the rice stem borer, *Chilo suppressalis* (Walker), and its ability to nucleate ice formation in supercooled water was also revealed [31]. Thus, we hypothesized that gut microbiome, especially INA bacteria and fungi are involved in the host physiological processes that also allow RTB larvae to survive under multiple pressures (e.g., cold and pathogens) during overwintering.

Reactive oxygen species (ROS) such as superoxide radicals (O_2^-), hydroxyl radical (OH^\cdot), H_2O_2 , and hydroperoxides ($ROOH$) are generated by exogenous and endogenous sources [32]. However, insects have evolved a complex antioxidant mechanism to overcome the toxic effects of ROS, including the activities of the SOD, CAT, and POD enzymes [33–35]. Lai et al. [36] suggested that when tissue metabolism in the moth *Evergestis extimalis* (Scopoli) decreases (to the point of being inhibited entirely at extremely low temperatures), the production of ROS in the tissues also decreases. In addition, they found that the activities of the protective enzymes POD, CAT, and SOD in *E. extimalis* larvae vary among seasons and are lowest in the coldest season [36]. Similarly, hemolymph CAT activity in larvae of the Mediterranean borer *Sesamia cretica* Lederer larvae is reduced significantly after cold exposure [37].

Although various aspects of the gut microbiome of the RTB have been investigated widely [38–44], it is unclear whether seasonal changes in temperature alter the composition of the gut microbiome, and if changes in the microbiome are interconnected with changes in the host physiology. We hypothesize that overwintering influences the composition of the gut microbiome of RTB, and these changes can have physiological consequences.

To explore how the microbiome conduces to the overwintering success of RTB larvae, we examined synchronous changes in the composition of the gut microbiome, cold tolerance, and the activities of antioxidant enzymes across different seasons. We found that the community of gut microbes in *D. valens* larvae changes with the season. In addition, we found that cold tolerance increases and the activities of the antioxidant enzymes catalase (CAT) and peroxidase (POD) decrease during the overwintering period. These synchronous changes in the composition of the gut microbiome and host physiology suggest that they may be interlinked, and that changes in the microbiome are connected with the overwintering success of *D. valens* larvae.

2. Materials and Methods

2.1. Bark Beetle Collection and Dissection

In 2019, mature larvae of *D. valens* were collected from galleries of the same host plant *Pinus tabulaeformis* Carrière using fine forceps in Heilihe town, located in Ningcheng County, Chifeng, Inner Mongolia Autonomous Region, China (41°24′35.82″ N, 118°27′49.31″ E) in autumn (September), winter (January), and spring (May). The mean monthly temperature and mean monthly minimum temperature in Ningcheng County are lowest in January [29]. Some of the collected larvae were placed in liquid nitrogen for quick-freezing and then transported to the laboratory and stored at −80 °C. Remaining larvae were transported alive to the laboratory in dark conditions for supercooling point (SCP) determination.

Before dissection, the larvae were disinfected superficially with 70% ethanol and then submerged repeatedly in phosphate-buffered saline solution to avoid external contamination. Subsequently, dissection and gut extraction were performed under sterile conditions on a laminar-flow clean bench, using an Olympus SZX10 stereomicroscope (Olympus Corporation, Tokyo, Japan). The guts were transferred individually to sterile 1.5 mL microcentrifuge tubes, immediately snap-frozen in liquid nitrogen, and stored at −80 °C until DNA extraction [38].

2.2. DNA Extraction, PCR Amplification, and Sequencing of Partial 16S rRNA and ITS Genes

In total, nine DNA samples (3 seasons × 3 replicated samples) were obtained. Five guts were pooled for each replicate and total genomic DNA was extracted using the DNeasy Blood and Tissue Kit (Qiagen, Valencia, CA, USA), according to the manufacturer's protocol. The obtained DNA was analyzed by Majorbio Bio-Pharm Technology Co., Ltd. (Shanghai, China). Specifically, the final DNA concentration and purification were determined using a NanoDrop 2000 UV-vis spectrophotometer (Thermo Scientific, Wilmington, NC, USA) and DNA quality was examined via 1% agarose gel electrophoresis.

Bacteria and fungi present in the samples were identified through 16S and ITS rRNA sequencing, respectively. For bacterial identification, the V3-V4 hypervariable regions of the bacterial 16S rRNA gene were amplified via PCR using the following primers: 338 F (5'-ACT CCT ACG GGA GGC AGC AG-3') and 806 R (5'-GGA CTA CHV GGG TWT CTA AT-3') [45,46]. For fungal identification, the ITS hypervariable regions were amplified with the following primers: ITS1F (5'-CTT GGT CAT TTA GAG GAA GTA A-3') [47] and ITS2R (5'-GCT GCG TTC TTC ATC GAT GC-3') [48]. PCRs were conducted using a GeneAmp 9700 thermocycler (Applied Biosystems, Foster City, CA, USA) and the following program: denaturation at 95 °C for 3 min, followed by 27 cycles of 95 °C for 30 s, 55 °C for 30 s, and 72 °C for 45 s, and then a final extension at 72 °C for 10 min. The resulting PCR products were extracted from a 2% agarose gel, purified using the AxyPrep DNA Gel Extraction Kit (Axygen Biosciences, Union City, CA, USA), and quantified using a QuantiFluor™-ST fluorometer (Promega, Madison, WI, USA), according to the manufac-

turers' protocols. Purified amplicons were pooled in equimolar amounts and paired-end sequenced (2×300 bp) using the Illumina MiSeq PE300 platform (Illumina, San Diego, CA, USA) at Majorbio Bio-Pharm Technology Co., Ltd., Shanghai, China.

2.3. Processing and Statistical Analysis of Sequencing Data

The sequencing data were processed using Quantitative Insights Into Microbial Ecology (QIIME, version 1.9.1), as described by Caporaso et al. [49]. Raw fastq files were demultiplexed, quality-filtered by Trimmomatic, and merged by FLASH with the following standards: (i) reads were truncated at any site receiving an average quality score < 20 over a 50 bp sliding window; (ii) primers were matched allowing two nucleotide mismatches, and reads containing ambiguous characters were discarded; and (iii) sequences with overlaps longer than 10 bp were merged according to their overlap sequence. Operational taxonomic units (OTUs) were clustered with a 97% similarity cutoff [50,51] using UPARSE (version 7.1), and chimeric sequences were identified and discarded using UCHIME [52]. The taxonomy of each 16S rRNA and ITS gene sequence was analyzed using the Ribosomal Database Project (RDP) Classifier algorithm (<http://rdp.cme.msu.edu/> (accessed on 10 November 2019)), comparing against the Silva (release 132; <http://www.arb-silva.de> (accessed on 10 November 2019)) 16S rRNA database and the UNITE (release 7.2; <http://unite.ut.ee/index.php> (accessed on 11 November 2019)) database, respectively. Because the sequencing depth varied across samples, we conducted a sub-sampling procedure to normalize the number of reads to the minimum observed across all samples (30,228 reads for the bacterial data and 54,335 reads for the fungal data) (Table S1) by subSeq [53], an open-source software package project for R version 4.0.1 (www.r-project.org (accessed on 6 August 2020)) [54].

The alpha diversity, or diversity within each community or sample, was determined using Mothur (version 1.30.2) to calculate the Observed species (count of unique species), Chao1 index (estimate of species richness), and Shannon index (estimate of species richness and evenness) metrics for each sample [49]. Rarefaction curves (graphs of each diversity metric vs. sequencing depth) were then generated up to the minimal observed sequencing depth (30,228 sequences for the bacterial data and 54,335 sequences for the fungal data). Beta diversity measures were calculated using QIIME [49]. Weighted and unweighted unifrac distances were subjected to principal coordinates analyses (PCoA) to identify and compare the microbial OTU abundances and associations between samples. All of these analyses were completed using the free online Majorbio Cloud Platform (www.majorbio.com (accessed on 5th September 2020)). Data visualization, including the barplot representation of the gut microbiota abundance at the family level, and Venn diagrams were also conducted using the Majorbio Cloud Platform.

2.4. Determination of the Supercooling Point

The supercooling point (SCP) of the larvae was determined using methods reported previously [55]. A thermocouple (TP100; SenYi, Nanjing, China) was placed against the cuticle of the middle of the larva, secured by wrapping the circumference of the larva with Parafilm (Bemis NA, Neenah, WI, USA), and linked to a data recorder (Model 4152; Yokogawa Electric Co., Seoul, Korea). Each larva was additionally wrapped with absorbent cotton and then placed into a high–low-temperature test chamber (GDW-100; YaShiLin, Beijing, China) and cooled from 20 °C to -35 °C at a rate of 1 °C/min. The body temperature of the larva was recorded throughout the process. The SCP is defined as the temperature at which insect body fluids cool to a certain extent and then begin to freeze. Subsequently, the body temperature increases suddenly, a change that is caused by the emission of latent heat of crystallization. Here, the SCP was identified as the flex point recorded by the thermocouple and computer. A total of 56 larvae (30 collected in January and 26 collected in September) were used to determine the SCP. Beeswarm was generated using the beeswarm package in R version 4.0.1 [54].

2.5. Antioxidant Enzyme Activity Assays

The activities of superoxide dismutase (SOD), peroxidase (POD), and catalase (CAT) in larvae collected in January and May were determined using commercially available standard assay kits (Nanjing Jiancheng Bioengineering Institute, Nanjing, China), according to the manufacturers' instructions. The kit used to measure SOD activity (A001) was based on xanthine oxidase, following the method of McCord and Fridovich [56]. The absorbance of the reaction mixtures was measured at 550 nm using a TU-1810 UV-vis spectrophotometer (Beijing Purkinje General Instrument Co., Ltd., Beijing, China). CAT activity was determined using a kit (A007-2) based on the method of Rao et al. [57], with H_2O_2 as a substrate. The absorbance of the reaction mixtures was measured at 405 nm. The activity of POD was measured using a kit (A084-4) based on the method of Chance and Maehly [58] and the absorbance of the reaction mixtures was measured at 420 nm. The protein content of the enzyme source was measured using the Bradford method and bovine serum albumin as the standard [59]. All enzyme activity is expressed as U/mg protein, where one unit represents the change in absorbance/min/mg protein. Due to limited samples collected in September, the larvae collected in January and May were used in antioxidant enzyme activity assays. Violin plots were generated using the *vioplot* package in R version 4.0.1 [54].

3. Results

3.1. Richness and Diversity Analysis

For bacteria, we obtained an average of $42,558 \pm 10,428$ (standard deviation) reads per sample, with a range of 30,228 to 57,422 (Table S1). We assigned these reads to 723 OTUs at a 97% sequence identity threshold. The number of bacterial OTUs per sample ranged from 34 to 300 (Table S1), with an average of 153 ± 106 per sample. For fungi, we obtained an average of $69,112 \pm 6509$ (standard deviation) reads per sample, with a range of 54,335 to 74,401 (Table S1). We assigned these reads to 169 OTUs at a 97% sequence identity threshold. Overall, the number of fungal OTUs per sample ranged from 19 to 68 (Table S1), with an average of 44 ± 16 per sample.

The rarefaction curves of the OTUs approached saturation (Figures S1a and S2a), suggesting that we captured most of the microbial diversity in each sample. The species richness of the gut bacteria (i.e., the total number of unique species per sample) was highest in January and lowest in May (Figure 1a and Figure S1b), whereas that of the gut fungi was highest in May and lowest in January (Figure 1b and Figure S2b). The diversity of the bacterial community was highest in January (i.e., the abundance of species was distributed more evenly among the number of species) and lowest in May (i.e., the abundance of species was dominated by few species) (Figure 1a and Figure S1c). By contrast, the diversity of the fungal community was highest in May and lowest in September (Figure 1b and Figure S2c). OTU-based PCoA analyses of the bacterial data using unweighted (Figure 1c) and weighted (Figure 1d) *uniFrac* dissimilarity matrices showed a clear separation of the samples collected in different seasons. Similar analyses of the fungal data (Figure 1e,f) also showed a clear separation of the samples collected in different seasons, with the exception of a few sporadic data points.

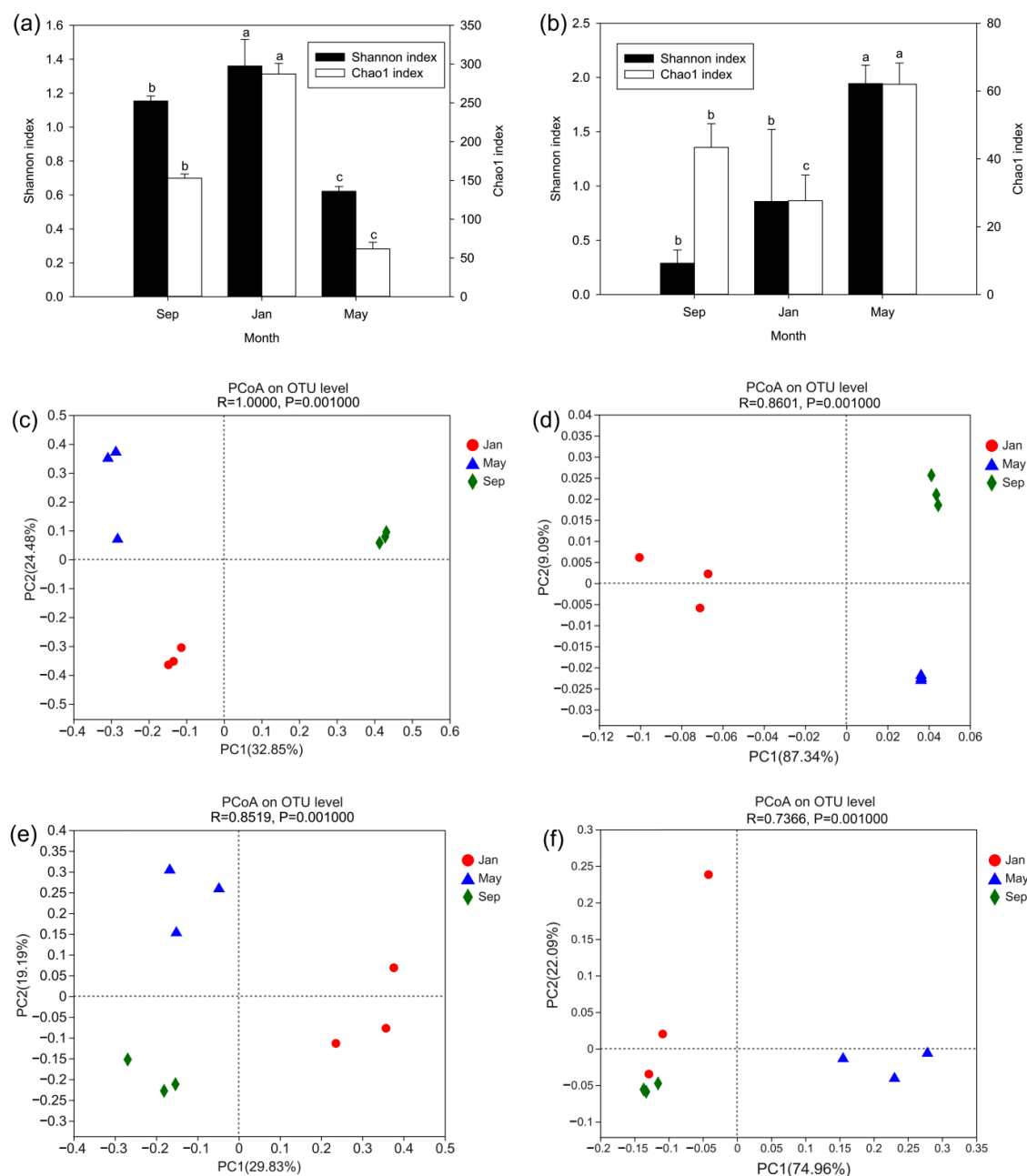


Figure 1. The species diversity and richness of the larval RTB gut microbiome across different seasons. (a,b) Species diversity (Shannon index) and richness (Chao1 index) measurements of the bacterial (a) and fungal (b) communities. Data are shown as the mean \pm standard deviation. Different lowercase letters represent significant differences between the groups ($p < 0.05$). (c–f) PCoA analyses of the bacterial (c,d) and fungal (e,f) OTUs using unweighted (c,e) and weighted (d,f) uniFrac dissimilarity matrices.

3.2. Taxonomic Profiling of the Bacterial Community

In January, the bacterial community of the larval RTB gut was dominated by Proteobacteria (the majority of which were in the genera *Erwinia*, *Serratia*, *Burkholderia*, and an unclassified genus within the family Enterobacteriaceae), followed by Bacteroidetes, Actinobacteria, and Firmicutes. Similarly, the bacterial community was also dominated by Proteobacteria in May and September; the majority of these bacteria identified in May were in the genera *Enterobacter*, *Erwinia*, and *Klebsiella*, whereas the majority of those identified in September were in the genera *Serratia*, *Enterobacter*, *Erwinia*, and *Klebsiella* (Figure 2a,b). The larvae collected in different seasons shared 17 genera of bacteria (Figure 2c), including

Enterobacter, *Serratia*, *Erwinia*, and *Klebsiella*. These genera are consistent with those reported by Hernández-García et al. [43] in their analysis of gut bacterial communities of RTB.

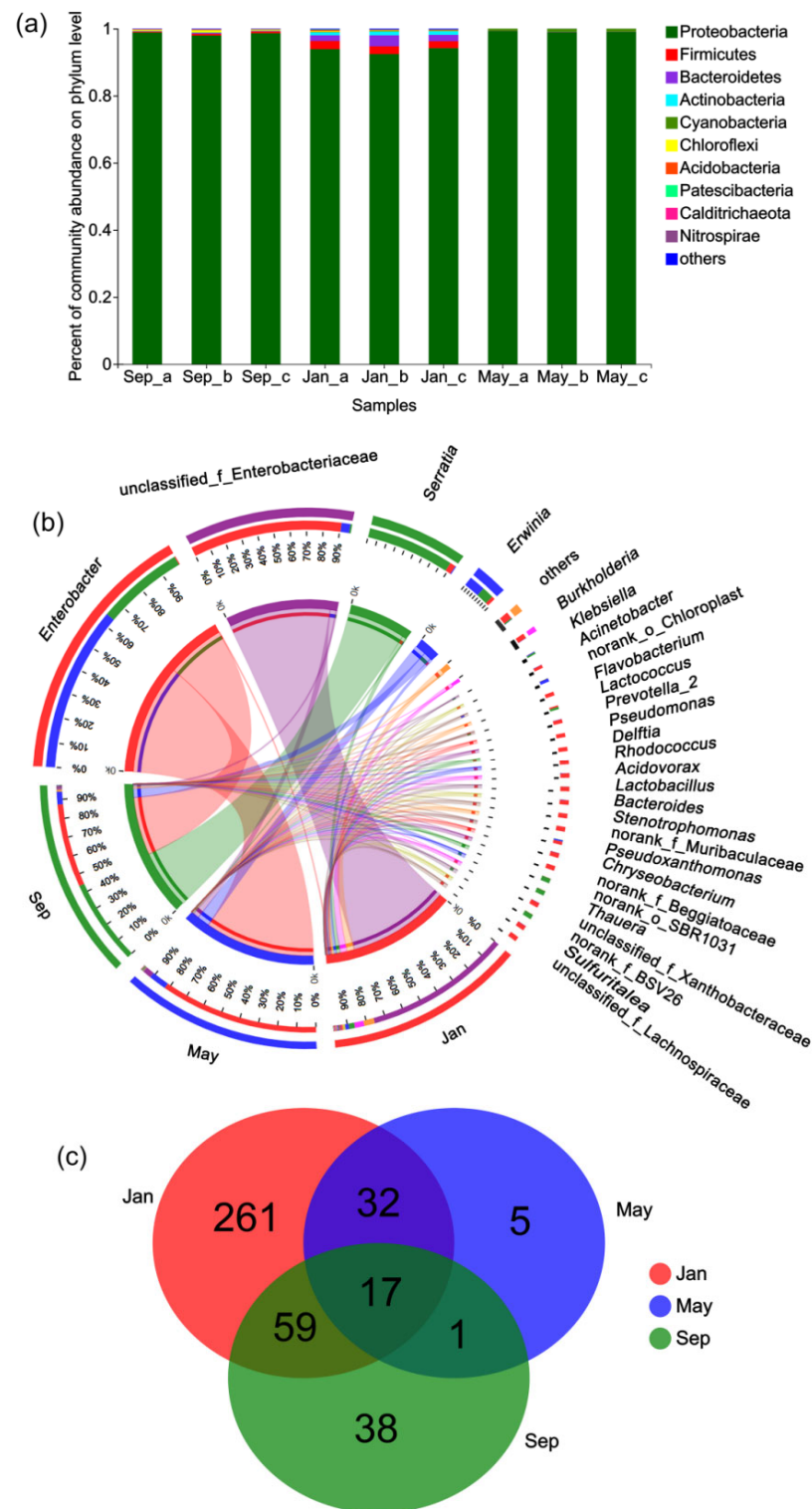


Figure 2. The diversity of the larval RTB gut microbiome across different seasons showing data for the bacterial communities. (a) The gut microbiota composition at the phylum level. (b) The gut microbiota composition at the genus level. (c) The numbers of common and unique genera found in the larvae collected in different seasons.

3.3. Taxonomic Profiling of the Fungal Community

In January, the fungal community of the larval RTB gut was dominated by Ascomycota (the majority of which were in the genera *Cyberlindnera* and *Candida*), followed by Basidiomycota. In May, the dominant gut fungi was also Ascomycota (the majority of which were in the genera *Cyberlindnera*, *Myxozyma*, *Penicillium*, *Myxozyma*, *Nakazawaea*, *Kuraishia*, *Candida*, *Ogataea*, and an unclassified genus within the order Saccharomycetales), followed by Chytridiomycota and Basidiomycota. Similarly, in September, the dominant gut fungi was also Ascomycota (the majority of which were in the genera *Cyberlindnera*) (Figure 3a,b). The larvae collected in different seasons shared 13 genera of fungi (Figure 3c), including *Cyberlindnera* and *Candida*. These two genera are consistent with those reported by Dohet et al. [40] in their analysis of fungal symbionts of RTB.

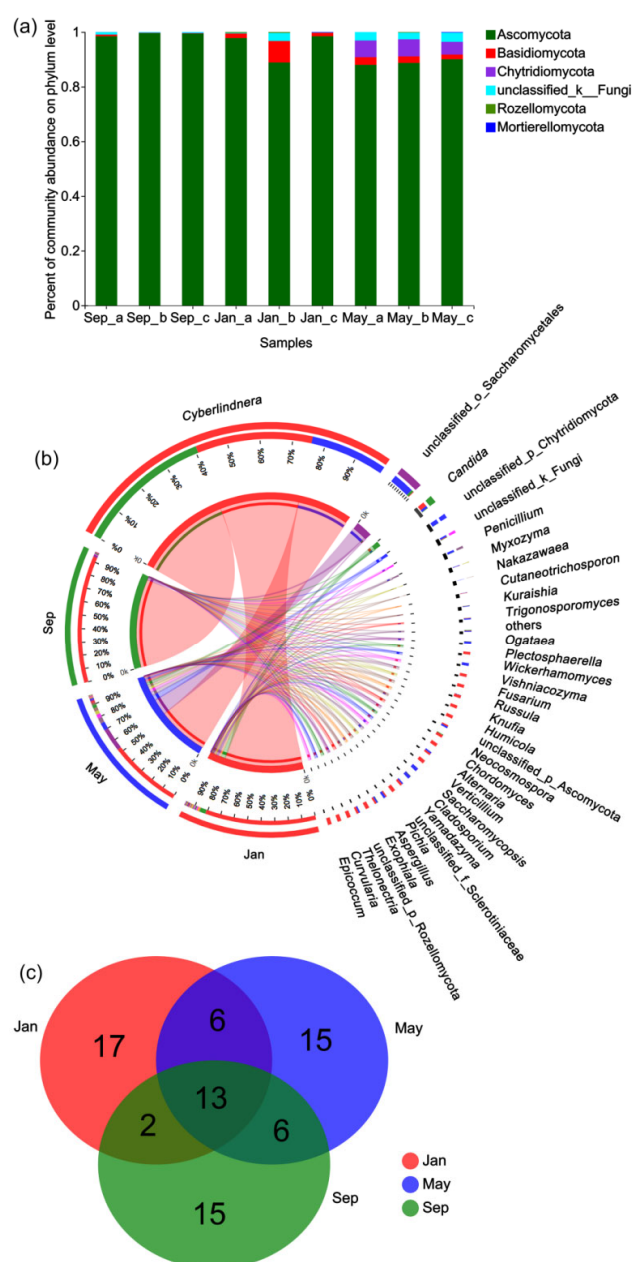


Figure 3. The diversity of the larval RTB gut microbiome across different seasons showing data for the fungal communities. (a) The gut microbiota composition at the phylum level. (b) The gut microbiota composition at the genus level. (c) The numbers of common and unique genera found in the larvae collected in different seasons.

3.4. Seasonal Changes in the Composition of the Gut Microbiome

Analyses of the bacterial data revealed that the genus *Enterobacter* displayed the greatest change across seasons, with relative abundances of approximately 44% in September, <1% in January, and approximately 84% in May (Figure 4a). By contrast, the unclassified genus within the family Enterobacteriaceae increased from <1% to almost 78% of the total bacterial abundance from September to January, and then fell to approximately 5% in May (Figure 4b). The abundances of two genera of facultative pathogens, *Serratia* and *Klebsiella* [60], also displayed seasonal changes in the gut. The relative abundance of *Serratia* decreased from approximately 45% to 3% from September to January, and then fell to <1% in May (Figure 4c). The genera *Klebsiella* comprised approximately 0.9% of the total bacterial abundance in September, but fell below detectable levels in January, before increasing to approximately 0.4% in May (Figure 4d). The abundance of the genera *Erwinia* decreased from approximately 7% to 2% from September to January, and then increased to approximately 9% in May (Figure 4e). In total, the abundance of the Enterobacteriaceae family decreased from approximately 98% to 84% from September to January, and then increased to approximately 99% in May (Figure 4f). In addition, the abundance of the genus *Burkholderia* increased from below a detectable level to approximately 4.5% from September to January, and then fell below the detectable level again in May (Figure 4g).

Analyses of the fungal data revealed that the relative abundance of the yeast *Cyberlindnera* decreased from approximately 96% to 83% from September to January, and then decreased further to approximately 52% in May (Figure 4h). The abundance of the yeast *Candida* increased from <1% to approximately 4% from September to January, and then fell to <1% in May (Figure 4i). In addition, the abundance of the yeast *Wickerhamomyces* was below detectable levels in September and January, but increased to approximately 0.8% in May (Figure 4j).

3.5. Seasonal Changes in the Cold Tolerance of *D. valens* Larvae

Next, to understand the cold resistance capacity of *D. valens*, we examined the SCPs of overwintering larvae. The mean SCP of larvae collected in January was significantly lower than that of larvae collected in September (January: -18.34 ± 1.45 °C, $n = 30$; September: -5.67 ± 2.32 °C, $n = 26$; Mann–Whitney U test: $z = -6.409$, $p < 0.001$; Figure 5).

3.6. Antioxidant Enzyme Activity

The activities of CAT ($t_{10} = -2.931$, $p < 0.05$, $n_{\text{Jan}} = 5$, $n_{\text{May}} = 7$; Figure 6a) and POD ($t_{13} = -3.832$, $p < 0.01$, $n_{\text{Jan}} = 7$, $n_{\text{May}} = 8$; Figure 6b) in larvae collected in January were significantly lower than those in larvae collected in May. By contrast, the activity of SOD ($t_{18} = -0.558$, $p = 0.583$, $n_{\text{Jan}} = 10$, $n_{\text{May}} = 10$; Figure 6c) did not differ significantly between the larvae collected in January and May.

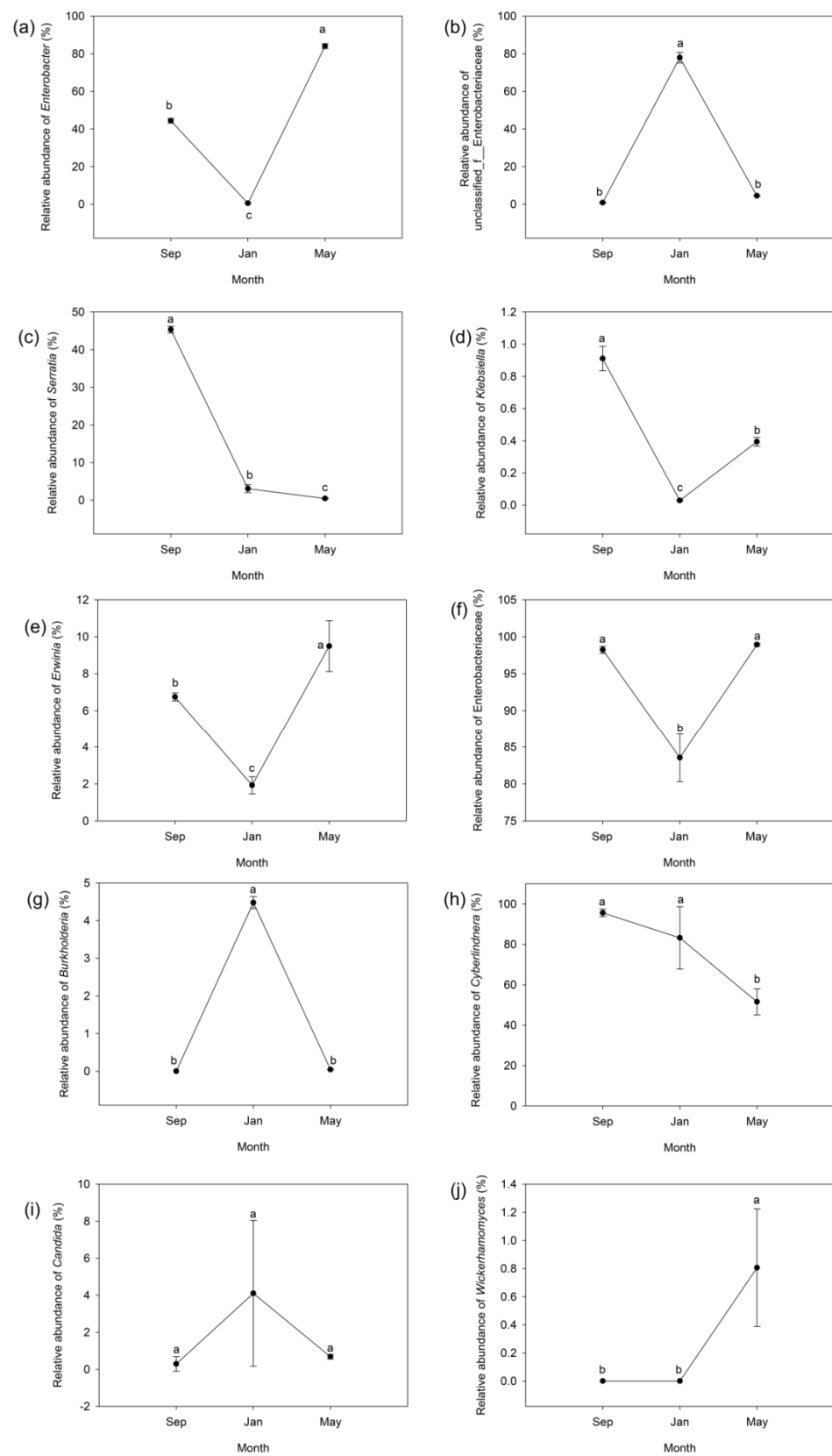


Figure 4. The relative abundances of the dominant microbial genera and families that showed the most variation across seasons. (a) *Enterobacter*, (b) unclassified_f_Enterobacteriaceae, (c) *Serratia*, (d) *Klebsiella*, (e) *Erwinia*, (f) Enterobacteriaceae, (g) *Burkholderia*, (h) *Cyberlindnera*, (i) *Candida*, (j) *Wickerhamomyces*. Results are shown as the mean \pm standard deviation.

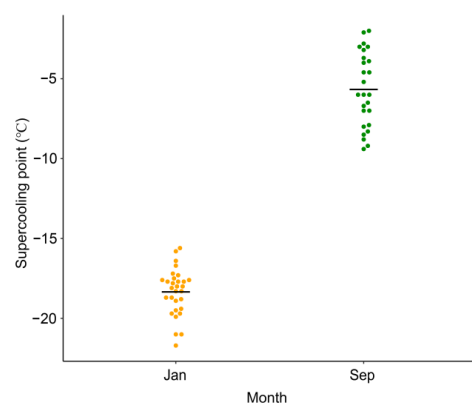


Figure 5. The supercooling points of larvae collected in January and September. Horizontal lines represent the means.

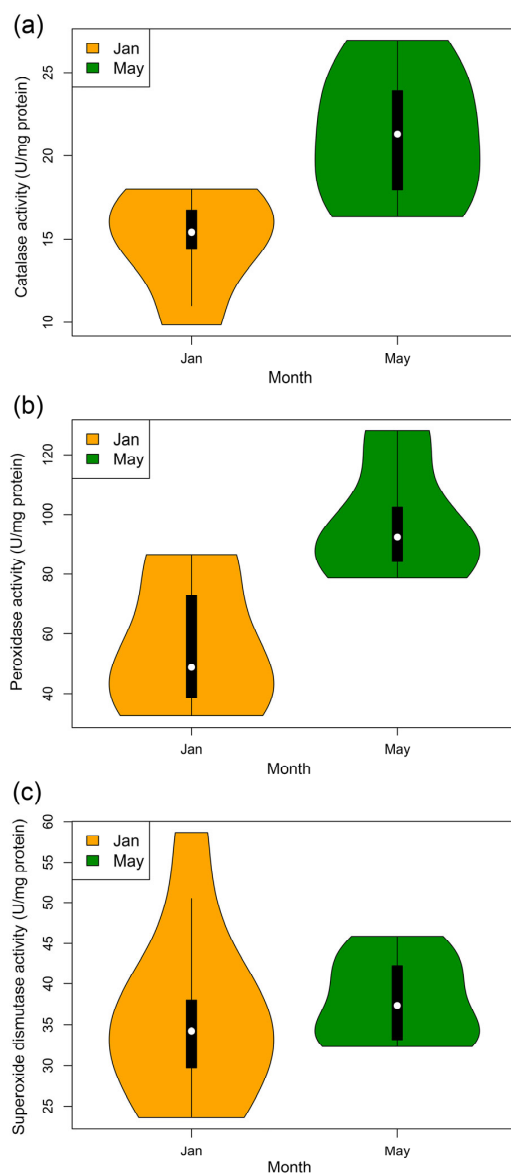


Figure 6. The activities of antioxidant enzymes in *D. valens* larvae collected in January and May. (a) Catalase activity. (b) Peroxidase activity. (c) Superoxide dismutase activity.

4. Discussion

Our findings presented here reveal that overwintering affects the compositions of the bacterial and fungal communities in the gut of *D. valens* larvae. Simultaneously, the cold tolerance of the larvae also appears to increase in the winter. The concurrent changes in the microbiome and host physiology suggest that the changes may be connected to involve in the overwintering success of *D. valens*.

Results showed that the activities of CAT and POD in *D. valens* larvae were significantly lower in January than in May. We propose that tissue metabolism in *D. valens* larvae is reduced in January; thus, the production of ROS in the tissues also decreases. ROS can also be produced by bacteria, such as the prevalent gut bacteria *Enterobacter* spp. [61]. In our current study, the relative abundance of *Enterobacter* was lowest in January (Figure 4a), suggesting a possible link between the amount of this genus of bacteria and the level of antioxidant enzyme activity in *D. valens* larvae.

INA bacteria include *Pantoea agglomerans* (Beijerinck) (synonyms: *Enterobacter agglomerans* (Beijerinck) Ewing and Fife, *Erwinia herbicola* (Löhnis) Dye) [30,62], *Enterobacter cancerogenus* (Urosevic) Dickey and Zumoff (also known as *Enterobacter taylorae* Farmer et al.) [30], *Erwinia* (*Pantoea*) *ananas* (Serrano) [63], and *Pseudomonas* spp. [28]. INA bacteria have been isolated from the lady beetle *Hippodamia convergens* Guérin-Ménéville [30], the bean leaf beetle *Cerotoma trifurcata* (Forster) [30], the diamondback moth *Plutella xylostella* (Linnaeus) [62], the mulberry pyralid *Glyphodes duplicalis* Inoue (formerly *Glyphodes pyloalis* Walker) [64], and the spring field cricket *G. veletis* [12]. Ingestion of INA bacteria increases the SCP of the lady beetle *H. convergens* [65] and ingestion of transgenic INA *Enterobacter cloacae* (Jordan) Hormaeche and Edwards reduces the cold-hardiness of corn borer and cotton bollworm larvae [66]. Lee et al. [30] suggested that the elimination of endogenous INA bacteria may be beneficial for freezing-intolerant insects for winter survival. In our current study, we observed seasonal variations in the abundances of a variety of taxa of bacteria; in particular, the abundances of *Enterobacter* (Figure 4a) and *Erwinia* (Figure 4e) decreased in the winter. As some species of these two genera are INA bacteria, we propose that their abundances in *D. valens* larvae may be regulated to control ice formation [7].

Many insects overwinter in chill coma or diapause with a slow metabolic rate and an inability to behaviorally defend against parasites and pathogens [67], suggesting that they may be susceptible to infection during overwintering. If hosts are threatened during overwintering by pathogens that enter via the gut [68], they would benefit from an active reduction in populations of these potential pathogens, such as bacteria of the genera *Enterobacter*, *Serratia*, and *Klebsiella*, which are frequently isolated, facultative insect pathogens [60]. Indeed, we observed a reduction in the abundances of *Enterobacter* (Figure 4a), *Serratia* (Figure 4c), and *Klebsiella* (Figure 4d) in the gut of *D. valens* larvae in January, indicating that these larvae may actively reduce the populations of potential pathogens in the gut when they are vulnerable during overwintering.

In addition to acting as facultative insect pathogens or ice nucleators, many species in the Enterobacteriaceae family contribute to insect nutrition, such as nitrogen fixation in the Queensland fruit fly *Bactrocera tryoni* (Froggatt) [69], the apple maggot fly *Rhagoletis pomonella* (Walsh) [70], and some termites [71]. Many insects, such as *G. veletis*, stop feeding but do not void their gut in the winter, which likely alters the available food and selects for bacteria capable of using whatever food is available [12]. Notably, in our current study, the abundance of the genus *Enterobacter* was reduced during overwintering, whereas that of the unclassified genus within the family Enterobacteriaceae was increased (Figure 4b). Our findings that Enterobacteriaceae was the dominant bacterial taxon in the gut and the abundances of the genera within Enterobacteriaceae varied across seasons suggest that *D. valens* larvae may actively regulate their gut microbiome to aid winter survival, for example by reducing the abundances of INA and facultative insect pathogens, while increasing those of harmless enterobacteria to optimize nutrition supply.

In addition to the functions mentioned above, members of the Enterobacteriaceae family also play a role in pheromone production; for example, *E. cloacae*, *Klebsiella pneu-*

monia (Schroeter) Trevisan, and *P. agglomerans* are involved in the production of locust cohesion pheromone [72]. In our current study, we found that the relative abundance of Enterobacteriaceae was highest (approximately 99% of the total abundance of bacteria) in May (Figure 4f). In addition, the abundances of *Enterobacter* (Figure 4a) and *Klebsiella* (Figure 4d) were higher in May than in January. Adult *D. valens* emerge and then spread to new hosts via a pheromone-mediated mass attack from mid-May to mid-June [42]. May is close to the time of eclosion; thus, the increases in the abundances of these bacteria may be related to the preparation for beetle pheromone production. In particular, the dominance of Enterobacteriaceae in the gut of larval *D. valens* suggests that they may be beneficial to host fitness, likely due to their abilities to hydrolyze and ferment carbohydrates, facilitate nitrogen fixation, and produce vitamins and pheromones [73].

Besides the Enterobacteriaceae family, many insect taxa participate in symbioses with the genus *Burkholderia*, a diverse group with members that can be mutualistic or pathogenic to plants, fungi, and animals [74]. *Burkholderia* symbionts can afford nutritional benefits and insecticide resistance to stinkbugs [75], allow *Lagria* beetle eggs to avoid pathogenic fungi infection [76], and may take part in nitrogen metabolism in ants [74]. Although the *Burkholderia* symbiont is not required for host survival, the aposymbiotic broad-headed bug *Riptortus clavatus* (Thunberg) and the bean bug *Riptortus pedestris* (Fabricius) grow slowly with smaller body size and weight, and lower fecundity than those of their symbiotic counterparts [77]. In the present study, the genus *Burkholderia* was detected in January (Figure 4g) but not May or September, suggesting that it may provide nutritional benefits to *D. valens* larvae and defend against pathogenic fungi in the winter.

During attack, bark beetles and associated microorganisms must overcome the complex defense system of the tree, which includes toxic monoterpenes, to successfully complete their life cycle. In this process, symbiont yeasts existing in the gut of bark beetles may take part in the detoxification of tree defensive chemicals [78]. For instance, the yeast *Cyberlindnera americana* (Wickerham) has been detected across different life stages and isolated from the body, ovarioles, and gut (where it is dominant) of *Dendroctonus* species from several geographical locations [15,79,80]. *Cyberlindnera americana* can degrade a number of substrates, including starch and lipids [80], and is a principal symbiont that resists high concentrations of monoterpenes (i.e., α -pinene) inside the gut of bark beetles [78]. In line with the previous report that this yeast is a common symbiont of *Dendroctonus* species [81], we identified *Cyberlindnera* as a dominant fungal genus in the gut of *D. valens* larvae, suggesting that it may help *D. valens* tolerate and degrade high amounts of tree defensive chemicals. In addition, Hernández-Martínez et al. [82] found that the symbiont yeast *Candida oregonensis* Phaff et do Carmo-Sousa may take part in the metabolism of terpenoids in the gut of the bark beetle *Dendroctonus rhizophagus* Thomas and Bright. We also detected *Candida* in the gut of *D. valens*, suggesting that it may play a similar role in the metabolism of terpenoids in this species.

The yeast *Wickerhamomyces* was also detected in the gut of *D. valens* larvae collected in May (Figure 4j). *Wickerhamomyces anomalus* (Hansen) Kurtzman et al. (also known as *Pichia anomala* (Hansen) Kurtzman or *Hansenula anomala* (Hansen) H. et P. Sydow) produces killer toxins with antimicrobial activity against fungi, including other yeasts, and bacteria [83]. The yeast *W. anomalus* was also isolated from arthropods, in particular, from *Drosophila* sp. [84], *Doubledaya bucculenta* Lewis beetles [85], and mosquitos [86]. One of the strains of *W. anomalus* isolated from the malaria mosquito vector *Anopheles stephensi* Liston produces a killer toxin that is active against other yeast species [87]. Due to its highly competitive inhibition of a variety of other microorganisms [88], *D. valens* larvae may use *W. anomalus* to control or defend against pathogens.

Overall, the results presented here show that the gut microbiome of *D. valens* changes during overwintering, and that these changes occur alongside changes in host physiology. The functional significance of these shifts in the microbiome requires further study, as they may contribute to the success of insect overwintering.

5. Conclusions

Overwintering resulted in changes to the gut microbiota of *Dendroctonus valens* larvae. In particular, the abundances of *Enterobacter*, *Serratia*, *Erwinia*, and *Klebsiella* decreased during overwintering. Concurrent with these changes, the cold resistance of *D. valens* larvae was enhanced, and the activities of the antioxidant enzymes catalase and peroxidase were reduced. Results suggest *D. valens* larvae may be confronted with multiple overwintering pressures, including pathogen pressure. It will be meaningful to confirm whether seasonal changes in the microbiome promote the success of host overwintering.

Supplementary Materials: The following are available online at <https://www.mdpi.com/article/10.3390/f12070888/s1>. Figure S1: Rarefaction plots for bacterial microbiomes in the gut of *Dendroctonus valens* across seasons, Figure S2: Rarefaction plots for fungal microbiomes in the gut of *D. valens* across seasons, Table S1: Summary of sequence number and operational taxonomic units (OTUs) in the gut microbiome of *D. valens*.

Author Contributions: Y.D., S.Z. and Z.H. designed the study. Y.D., Z.H., F.S., S.G. and Y.X. collected the data. Y.D. and Z.H. performed data analyses. Z.H., S.Z., J.T. and L.R. wrote the manuscript. All authors have read and agreed to the published version of the manuscript.

Funding: This study was funded by the Fundamental Research Funds for the Central Universities (Grant No. BLX201902) (for Z.H.), and the National Key Research and Development Program of China (2018YFD0600200) (for S.Z.).

Institutional Review Board Statement: Not applicable.

Informed Consent Statement: Not applicable.

Data Availability Statement: The raw reads generated and analyzed in this study were deposited in the National Center for Biotechnology Information (NCBI) Sequence Read Archive (SRA) database (BioProject ID: PRJNA704720).

Acknowledgments: We would like to express our deep gratitude to Dongfang Zhao and Chun Chun Zheng (Beijing Forestry University, China) for their help with specimen collection.

Conflicts of Interest: The authors declare that they have no conflict of interest.

References

- Engel, P.; Moran, N.A. The gut microbiota of insects—diversity in structure and function. *FEMS Microbiol. Rev.* **2013**, *37*, 699–735. [\[CrossRef\]](#)
- Douglas, A.E. Multiorganismal insects: Diversity and function of resident microorganisms. *Annu. Rev. Entomol.* **2015**, *60*, 17–34. [\[CrossRef\]](#)
- Shin, S.C.; Kim, S.H.; You, H.; Kim, B.; Kim, A.C.; Lee, K.A.; Yoon, J.H.; Ryu, J.H.; Lee, W.J. *Drosophila* microbiome regulates modulates host development and homeostasis via insulin signaling. *Science* **2011**, *334*, 670–674. [\[CrossRef\]](#)
- Ge, S.; Shi, F.; Pei, J.; Hou, Z.; Zong, S.; Ren, L. Gut Bacteria Associated With *Monochamus saltuarius* (Coleoptera: Cerambycidae) and Their Possible Roles in Host Plant Adaptations. *Front. Microbiol.* **2021**, *12*, 687211. [\[CrossRef\]](#)
- Williams, C.M.; Henry, H.A.; Sinclair, B.J. Cold truths: How winter drives responses of terrestrial organisms to climate change. *Biol. Rev.* **2015**, *90*, 214–235. [\[CrossRef\]](#) [\[PubMed\]](#)
- Hahn, D.A.; Denlinger, D.L. Meeting the energetic demands of insect diapause: Nutrient storage and utilization. *J. Insect Physiol.* **2007**, *53*, 760–773. [\[CrossRef\]](#) [\[PubMed\]](#)
- Olsen, T.M.; Duman, J.G. Maintenance of the supercooled state in overwintering pyrochroid beetle larvae, *Dendroides canadensis*: Role of hemolymph ice nucleators and antifreeze proteins. *J. Comp. Physiol. B* **1997**, *167*, 105–113. [\[CrossRef\]](#)
- Ferguson, L.V.; Sinclair, B.J. Insect immunity varies idiosyncratically during overwintering. *J. Exp. Zool. Part A* **2017**, *327*, 222–234. [\[CrossRef\]](#) [\[PubMed\]](#)
- Denlinger, D.L.; Lee, R.E. *Low Temperature Biology of Insects*; Cambridge University Press: Cambridge, UK, 2010.
- Carey, H.V.; Duddleston, K.N. Animal-microbial symbioses in changing environments. *J. Therm. Biol.* **2014**, *44*, 78–84. [\[CrossRef\]](#)
- Wang, J.; Chen, H.; Tang, M. Community structure of gut bacteria of *Dendroctonus armandi* (Coleoptera: Curculionidae: Scolytinae) larvae during overwintering stage. *Sci. Rep.* **2017**, *7*, 14242. [\[CrossRef\]](#)
- Ferguson, L.V.; Dhakal, P.; Lebenzon, J.E.; Heinrichs, D.E.; Bucking, C.; Sinclair, B.J. Seasonal shifts in the insect gut microbiome are concurrent with changes in cold tolerance and immunity. *Funct. Ecol.* **2018**, *32*, 2357–2368. [\[CrossRef\]](#)
- Owen, D.R.; Smith, S.L.; Seybold, S.J. *Red turpentine beetle. Forest Insect & Disease Leaflet*; US Department of Agriculture, Forest Service: Washington, DC, USA, 2010; Volume 55, pp. 1–8.

14. Sun, J.; Lu, M.; Gillette, N.E.; Wingfield, M.J. Red turpentine beetle: Innocuous native becomes invasive tree killer in China. *Annu. Rev. Entomol.* **2013**, *58*, 293–311. [\[CrossRef\]](#)
15. Lou, Q.Z.; Lu, M.; Sun, J.H. Yeast diversity associated with invasive *Dendroctonus valens* killing *Pinus tabulaeformis* in China using cultural and molecular methods. *Microb. Ecol.* **2014**, *68*, 397–415. [\[CrossRef\]](#) [\[PubMed\]](#)
16. Miao, Z.W.; Chou, W.M.; Huo, F.Y.; Wang, X.L.; Fang, J.X.; Zhao, M.M. Biology of *Dendroctonus valens* in Shanxi Province. *Shanxi For. Sci. Technol.* **2001**, *23*, 34–37. (In Chinese)
17. Zhan, Z.; Yu, L.; Li, Z.; Ren, L.; Gao, B.; Wang, L.; Luo, Y. Combining GF-2 and Sentinel-2 images to detect tree mortality caused by red turpentine beetle during the early outbreak stage in north China. *Forests* **2020**, *11*, 172. [\[CrossRef\]](#)
18. Zheng, C.; Zhao, D.; Xu, Y.; Shi, F.; Zong, S.; Tao, J. Reference gene selection for expression analyses by qRT-PCR in *Dendroctonus valens*. *Insects* **2020**, *11*, 328. [\[CrossRef\]](#)
19. Zhao, D.; Zheng, C.; Shi, F.; Xu, Y.; Zong, S.; Tao, J. Expression analysis of genes related to cold tolerance in *Dendroctonus valens*. *PeerJ* **2021**, *9*, e10864. [\[CrossRef\]](#)
20. Yan, Z.; Sun, J.H.; Don, O.; Zhang, Z. The red turpentine beetle, *Dendroctonus valens* LeConte (Scolytidae): An exotic invasive pest of pine in China. *Biodivers. Conserv.* **2005**, *14*, 1735–1760. [\[CrossRef\]](#)
21. Xu, L.T.; Lu, M.; Sun, J.H. Invasive bark beetle-associated microbes degrade a host defensive monoterpene. *Insect Sci.* **2016**, *23*, 183–190. [\[CrossRef\]](#)
22. He, S.Y.; Ge, X.Z.; Wang, T.; Wen, J.B.; Zong, S.X. Areas of potential suitability and survival of *Dendroctonus valens* in China under extreme climate warming scenario. *Bull. Entomol. Res.* **2015**, *105*, 477–484. [\[CrossRef\]](#)
23. Lu, M.; Zhou, X.D.; de Beer, Z.W.; Wingfield, M.J.; Sun, J.H. Ophiostomatoid fungi associated with the invasive pine-infesting bark beetle, *Dendroctonus valens*, in China. *Fungal Divers.* **2009**, *38*, 133–145.
24. Liu, F.; Wickham, J.D.; Cao, Q.; Lu, M.; Sun, J. An invasive beetle-fungus complex is maintained by fungal nutritional-compensation mediated by bacterial volatiles. *ISME J.* **2020**, *14*, 2829–2842. [\[CrossRef\]](#) [\[PubMed\]](#)
25. Marincowitz, S.; Duong, T.A.; Taerum, S.J.; de Beer, Z.W.; Wingfield, M.J. Fungal associates of an invasive Pine—Infesting bark beetle, *Dendroctonus valens*, including seven new Ophiostomatalean fungi. *Persoonia* **2020**, *45*, 177–195. [\[CrossRef\]](#)
26. Cannon, R.J.C.; Block, W. Cold tolerance of microarthropods. *Biol. Rev.* **1988**, *63*, 23–77. [\[CrossRef\]](#)
27. Lee, R. Principles of insect low temperature tolerance. In *Insects at Low Temperature*; Lee, R., Denlinger, D., Eds.; Springer: Berlin/Heidelberg, Germany, 1991; pp. 17–46.
28. Lee, R.E.; Lee, M.R.; Strong-Gunderson, J.M. Insect cold-hardiness and ice nucleating active microorganisms including their potential use for biological control. *J. Insect Physiol.* **1993**, *39*, 1–12. [\[CrossRef\]](#)
29. Dong, Y.; Pei, J.; Shao, Y.; Zong, S.; Hou, Z. Cold tolerance and cold tolerant substances of larva and adult of *Dendroctonus valens* LeConte (Coleoptera). *J. Environ. Entomol.* **2021**, (in press). [\[CrossRef\]](#)
30. Lee, R.E.; Strong-Gunderson, J.M.; Lee, M.R.; Grove, K.S.; Riga, T.J. Isolation of ice nucleating active bacteria from insects. *J. Exp. Zool.* **1991**, *257*, 124–127. [\[CrossRef\]](#)
31. Tsumuki, H.; Konno, H.; Maeda, T.; Okamoto, Y. An ice-nucleating active fungus isolated from the gut of the rice stem borer, *Chilo suppressalis* Walker (Lepidoptera: Pyralidae). *J. Insect Physiol.* **1992**, *38*, 119–125. [\[CrossRef\]](#)
32. Ahmad, R.S.; Pardini, R.S. Mechanisms for regulating oxygen toxicity in phytophagous insects. *Free Radic. Biol. Med.* **1990**, *8*, 401–413. [\[CrossRef\]](#)
33. Barbehenn, R.V. Gut-based antioxidant enzymes in a polyphagous and a graminivorous grasshopper. *J. Chem. Ecol.* **2002**, *28*, 1329–1347. [\[CrossRef\]](#)
34. Hou, Z.; Wei, C. *De novo* comparative transcriptome analysis of a rare cicada, with identification of candidate genes related to adaptation to a novel host plant and drier habitats. *BMC Genom.* **2019**, *20*, 182. [\[CrossRef\]](#) [\[PubMed\]](#)
35. Hou, Z.; Shi, F.; Ge, S.; Tao, J.; Ren, L.; Wu, H.; Zong, S. Comparative transcriptome analysis of the newly discovered insect vector of the pine wood nematode in China, revealing putative genes related to host plant adaptation. *BMC Genom.* **2021**, *22*, 189. [\[CrossRef\]](#)
36. Lai, Y.P.; Tao, K.; Hou, T.P. Preliminary analysis of geographical distribution based on cold hardiness for *Evergestis extimalis* (Scopoli) (Lepidoptera:Pyralidae) on Qinghai-Tibet Plateau. *Entomol. Res.* **2019**, *49*, 13–20. [\[CrossRef\]](#)
37. Grubor-Lajsic, G.; Block, W.; Telesmanic, M.; Javanovic, A.; Stevanovic, D.; Baca, F. Effect of cold acclimation on the antioxidant defense system of two larval *Lepidoptera* (Noctuidae). *Arch. Insect Biochem. Physiol.* **1997**, *36*, 1–10. [\[CrossRef\]](#)
38. Morales-Jiménez, J.; Zúñiga, G.; Villa-Tanaca, L.; Hernández-Rodríguez, C. Bacterial community and nitrogen fixation in the red turpentine beetle, *Dendroctonus valens* LeConte (Coleoptera: Curculionidae: Scolytinae). *Microb. Ecol.* **2009**, *58*, 879–891. [\[CrossRef\]](#) [\[PubMed\]](#)
39. Adams, A.S.; Adams, S.M.; Currie, C.R.; Gillette, N.E.; Raffa, K.F. Geographic variation in bacterial communities associated with the red turpentine beetle (Coleoptera: Curculionidae). *Environ. Entomol.* **2010**, *39*, 406–414. [\[CrossRef\]](#) [\[PubMed\]](#)
40. Dohet, L.; Grégoire, J.C.; Berasategui, A.; Kaltenpoth, M.; Biedermann, P.H.W. Bacterial and fungal symbionts of parasitic *Dendroctonus* bark beetles. *FEMS Microbiol. Ecol.* **2016**, *92*, fiw129. [\[CrossRef\]](#)
41. Hernández-García, J.A.; Briones-Roblero, C.I.; Rivera-Orduña, F.N.; Zúñiga, G. Revealing the gut bacteriome of *Dendroctonus* bark beetles (Curculionidae: Scolytinae): Diversity, core members and co-evolutionary patterns. *Sci. Rep.* **2017**, *7*, 13864. [\[CrossRef\]](#)
42. Cao, Q.; Wickham, J.D.; Chen, L.; Ahmad, F.; Lu, M.; Sun, J. Effect of oxygen on verbenone conversion from cis-verbenol by gut facultative anaerobes of *Dendroctonus valens*. *Front. Microbiol.* **2018**, *9*, 464. [\[CrossRef\]](#)

43. Hernández-García, J.A.; Gonzalez-Escobedo, R.; Briones-Roblero, C.I.; Cano-Ramírez, C.; Rivera-Orduña, F.N.; Zúñiga, G. Gut bacterial communities of *Dendroctonus valens* and *D. mexicanus* (Curculionidae: Scolytinae): A metagenomic analysis across different geographical locations in Mexico. *Int. J. Mol. Sci.* **2018**, *19*, 2578. [\[CrossRef\]](#) [\[PubMed\]](#)
44. Xu, D.; Xu, L.; Zhou, F.; Wang, B.; Wang, S.; Lu, M.; Sun, J. Gut bacterial communities of *Dendroctonus valens* and monoterpenes and carbohydrates of *Pinus tabulaeformis* at different attack densities to host pines. *Front. Microbiol.* **2018**, *9*, 1251. [\[CrossRef\]](#)
45. Zhang, Y.K.; Yu, Z.J.; Wang, D.; Bronislava, V.; Branislav, P.; Liu, J.Z. The bacterial microbiome of field-collected *Dermacentor marginatus* and *Dermacentor reticulatus* from Slovakia. *Parasit. Vectors* **2019**, *12*, 325. [\[CrossRef\]](#) [\[PubMed\]](#)
46. Liang, S.; Wang, C.; Ahmad, F.; Yin, X.; Hu, Y.; Mo, J. Exploring the effect of plant substrates on bacterial community structure in termite fungus-combs. *PLoS ONE* **2020**, *15*, e0232329. [\[CrossRef\]](#) [\[PubMed\]](#)
47. Gardes, M.; Bruns, T.D. ITS primers with enhanced specificity for Basidiomycetes—Application to the identification of mycorrhizae and rusts. *Mol. Ecol.* **1993**, *2*, 113–118. [\[CrossRef\]](#) [\[PubMed\]](#)
48. White, T.J.; Bruns, T.D.; Lee, S.B.; Taylor, J.W. Amplification and direct sequencing of fungal ribosomal RNA genes for phylogenetics. In *PCR Protocols: A Guide to Methods and Applications*; Innis, M.A., Gelfand, D.H., Sninsky, J.J., White, T.J., Eds.; Academic Press: Cambridge, MA, USA, 1990; pp. 315–322.
49. Caporaso, J.G.; Bittinger, K.; Bushman, F.D.; DeSantis, T.Z.; Andersen, G.L.; Knight, R. PyNAST: A flexible tool for aligning sequences to a template alignment. *Bioinformatics* **2010**, *26*, 266–267. [\[CrossRef\]](#)
50. Stackebrandt, E.; Goebel, B.M. Taxonomic note: A place for DNA–DNA reassociation and 16S rRNA sequence analysis in the present species definition in bacteriology. *Int. J. Syst. Evol. Microbiol.* **1994**, *44*, 846–849. [\[CrossRef\]](#)
51. Edgar, R.C. UPARSE: Highly accurate OTU sequences from microbial amplicon reads. *Nat. Methods* **2013**, *10*, 996–998. [\[CrossRef\]](#)
52. Edgar, R.C.; Haas, B.J.; Clemente, J.C.; Quince, C.; Knight, R. UCHIME improves sensitivity and speed of chimera detection. *Bioinformatics* **2011**, *27*, 2194–2200. [\[CrossRef\]](#)
53. Robinson, D.G.; Storey, J.D. subSeq: Determining appropriate sequencing depth through efficient read subsampling. *Bioinformatics* **2014**, *30*, 3424–3426. [\[CrossRef\]](#)
54. R Core Team. *R: A Language and Environment for Statistical Computing*; R Foundation for Statistical Computing: Vienna, Austria, 2018.
55. Feng, Y.; Tursun, R.; Xu, Z.; Ouyang, F.; Zong, S. Effect of three species of host tree on the cold hardiness of overwintering larvae of *Anoplophora glabripennis* (Coleoptera: Cerambycidae). *Eur. J. Entomol.* **2016**, *113*, 212–216. [\[CrossRef\]](#)
56. McCord, J.M.; Fridovich, I. Superoxide dismutase: An enzymic function for erythrocuprein (hemocuprein). *J. Biol. Chem.* **1969**, *244*, 6049–6055. [\[CrossRef\]](#)
57. Rao, M.V.; Paliyath, G.; Ormrod, D.P. Ultraviolet B and ozone induced biochemical changes in antioxidant enzymes of *Arabidopsis thaliana*. *Plant. Physiol.* **1996**, *110*, 125–136. [\[CrossRef\]](#)
58. Chance, B.; Maehly, A.C. Assay of catalase and peroxidases. *Meth. Enzymol.* **1955**, *2*, 764–775.
59. Bradford, M. A rapid and sensitive method for the quantitation of microgram quantities of protein utilizing the principle of protein-dye binding. *Anal. Biochem.* **1976**, *72*, 248–254. [\[CrossRef\]](#)
60. Lysenko, O. Non-sporeforming bacteria pathogenic to insects: Incidence and mechanisms. *Annu. Rev. Microbiol.* **1985**, *39*, 673–695. [\[CrossRef\]](#) [\[PubMed\]](#)
61. Cirimotich, C.M.; Dong, Y.; Clayton, A.M.; Sandiford, S.L.; Souza-Neto, J.A.; Mulenga, M.; Dimopoulos, G. Natural microbe-mediated refractoriness to *Plasmodium* infection in *Anopheles gambiae*. *Science* **2011**, *332*, 855–858. [\[CrossRef\]](#) [\[PubMed\]](#)
62. Kaneko, J.; Yoshida, T.; Owada, T.; Kita, K.; Tanno, K. *Erwinia herbicola*: Ice nucleation active bacteria isolated from diamondback moth, *Plutella xylostella* L. pupae. *Jpn. J. Appl. Entomol. Z.* **1991**, *35*, 247–251. [\[CrossRef\]](#)
63. Watanabe, K.; Sato, M. Gut colonization by an ice nucleation active bacterium, *Erwinia (Pantoea) ananas* reduces the cold hardiness of mulberry pyralid larvae. *Cryobiology* **1999**, *38*, 281–289. [\[CrossRef\]](#)
64. Takahashi, K.; Watanabe, K.; Sato, M. Survival and characteristics of ice nucleation-active bacteria on Mulberry trees (*Morus* spp.) and in Mulberry pyralid (*Glyphodes pyloalis*). *Ann. Phytopathol. Soc. Jpn.* **1995**, *61*, 439–443. [\[CrossRef\]](#)
65. Strong-Gunderson, J.M.; Lee, R.E.; Lee, M.R.; Riga, T.J. Ingestion of ice nucleating active bacteria increases the supercooling point of the lady beetle *Hippodamia convergens*. *J. Insect Physiol.* **1990**, *36*, 153–157. [\[CrossRef\]](#)
66. Tang, C.; Sun, F.; Zhang, X.; Zhao, T.; Qi, J. Transgenic ice nucleation-active *Enterobacter cloacae* reduces cold hardiness of corn borer and cotton bollworm larvae. *FEMS Microbiol. Ecol.* **2004**, *51*, 79–86. [\[CrossRef\]](#)
67. Rider, M.H.; Hussain, N.; Dilworth, S.M.; Storey, J.M.; Storey, K.B. AMP-activated protein kinase and metabolic regulation in cold-hardy insects. *J. Insect Physiol.* **2011**, *57*, 1453–1462. [\[CrossRef\]](#) [\[PubMed\]](#)
68. Sinclair, B.J.; Ferguson, L.V.; Salehipour-shirazi, G.; MacMillan, H.A. Cross-tolerance and cross-talk in the cold: Relating low temperatures to desiccation and immune stress in insects. *Integr. Comp. Biol.* **2013**, *53*, 545–556. [\[CrossRef\]](#)
69. Murphy, K.M.; Teakle, D.S.; Macrae, I.C. Kinetics of colonization of adult Queensland fruit-flies *Bactrocera tryoni* by dinitrogen-fixing alimentary-tract bacteria. *Appl. Environ. Microbiol.* **1994**, *60*, 2508–2517. [\[CrossRef\]](#) [\[PubMed\]](#)
70. Lauzon, C.R.; Bussert, T.G.; Sjogren, R.E.; Prokopy, R.J. *Serratia marcescens* as a bacterial pathogen of *Rhagoletis pomonella* flies (Diptera: Tephritidae). *Eur. J. Entomol.* **2003**, *100*, 87–92. [\[CrossRef\]](#)
71. Ohkuma, M.; Noda, S.; Kudo, T. Phylogenetic diversity of nitrogen fixation genes in the symbiotic microbial community in the gut of diverse termites. *Appl. Environ. Microbiol.* **1999**, *65*, 4926–4934. [\[CrossRef\]](#)

72. Dillon, R.J.; Vennard, C.T.; Charnley, A.K. A Note: Gut bacteria produce components of a locust cohesion pheromone. *J. Appl. Microbiol.* **2002**, *92*, 759–763. [[CrossRef](#)] [[PubMed](#)]
73. Rizzi, A.; Crotti, E.; Borruso, L.; Jucker, C.; Lupi, D.; Colombo, M.; Daffonchio, D. Characterization of the bacterial community associated with larvae and adults of *Anoplophora chinensis* collected in Italy by culture and culture-independent methods. *BioMed. Res. Int.* **2013**, *2013*, 420287. [[CrossRef](#)] [[PubMed](#)]
74. Kaltenpoth, M.; Flórez, L.V. Versatile and dynamic symbioses between insects and *Burkholderia* bacteria. *Annu. Rev. Entomol.* **2020**, *65*, 145–170. [[CrossRef](#)] [[PubMed](#)]
75. Kikuchi, Y.; Hosokawa, T.; Fukatsu, T. An ancient but promiscuous host-symbiont association between *Burkholderia* gut symbionts and their heteropteran hosts. *ISME J.* **2011**, *5*, 446–460. [[CrossRef](#)] [[PubMed](#)]
76. Flórez, L.V.; Kaltenpoth, M. Symbiont dynamics and strain diversity in the defensive mutualism between *Lagri* beetles and *Burkholderia*. *Environ. Microbiol.* **2017**, *19*, 3674–3688. [[CrossRef](#)]
77. Takeshita, K.; Kikuchi, Y. *Riptortus pedestris* and *Burkholderia* symbiont: An ideal model system for Insect—Microbe symbiotic associations. *Res. Microbiol.* **2017**, *168*, 175–187. [[CrossRef](#)] [[PubMed](#)]
78. Soto-Robles, L.V.; Torres-Banda, V.; Rivera-Orduña, F.N.; Curiel-Quesada, E.; Hidalgo-Lara, M.E.; Zúñiga, G. An overview of genes from *Cyberlindnera americana*, a symbiont yeast isolated from the gut of the bark beetle *Dendroctonus rhizophagus* (Curculionidae: Scolytinae), involved in the detoxification process using genome and transcriptome data. *Front. Microbiol.* **2019**, *10*, 2180. [[CrossRef](#)] [[PubMed](#)]
79. Rivera, F.N.; González, E.; Gómez, Z.; López, N.; Hernández-Rodríguez, C.; Berkov, A.; Zúñiga, G. Gut—Associated yeast in bark beetles of the genus *Dendroctonus* Erichson (Coleoptera: Curculionidae: Scolytinae). *Biol. J. Linn. Soc.* **2009**, *98*, 325–342. [[CrossRef](#)]
80. Briones-Roblero, C.I.; Rodríguez-Díaz, R.; Santiago-Cruz, J.A.; Zúñiga, G.; Rivera-Orduña, F.N. Degradation capacities of bacteria and yeasts isolated from the gut of *Dendroctonus rhizophagus* (Curculionidae: Scolytinae). *Folia. Microbiol.* **2017**, *62*, 1–9. [[CrossRef](#)] [[PubMed](#)]
81. Davis, T.S. The ecology of yeast in the bark beetle holobiont: A century of research revisited. *Microb. Ecol.* **2015**, *69*, 723–732. [[CrossRef](#)] [[PubMed](#)]
82. Hernández-Martínez, F.; Briones-Roblero, C.I.; Nelson, D.R.; Rivera-Orduña, F.N.; Zúñiga, G. Cytochrome P450 complement (CYPome) of *Candida oregonensis*, a gut-associated yeast of bark beetle, *Dendroctonus rhizophagus*. *Fungal Biol.* **2016**, *120*, 1077–1089. [[CrossRef](#)] [[PubMed](#)]
83. Passoth, V.; Olstorpe, M.; Schnürer, J. Past, present and future research directions with *Pichia anomala*. *Antonie Van Leeuwenhoek* **2011**, *99*, 121–125. [[CrossRef](#)]
84. Zacchi, L.; Vaughan-Martini, A. Yeasts associated with insects in agricultural areas of Perugia, Italy. *Ann. Microbiol.* **2002**, *52*, 237–244.
85. Toki, W.; Tanahashi, M.; Togashi, K.; Fukatsu, T. Fungal farming in a non-social beetle. *PLoS ONE* **2012**, *7*, e41893. [[CrossRef](#)]
86. Ricci, I.; Mosca, M.; Valzano, M.; Damiani, C.; Scuppa, P.; Rossi, P.; Crotti, E.; Cappelli, A.; Ulissi, U.; Capone, A.; et al. Different mosquito species host *Wickerhamomyces anomalus* (*Pichia anomala*): Perspectives on vector-borne diseases symbiotic control. *Antonie Van Leeuwenhoek* **2011**, *99*, 43–50. [[CrossRef](#)] [[PubMed](#)]
87. Cappelli, A.; Ulissi, U.; Valzano, M.; Damiani, C.; Epis, S.; Gabrielli, M.G.; Conti, S.; Polonelli, L.; Bandi, C.; Favia, G.; et al. A *Wickerhamomyces anomalus* killer strain in the malaria vector *Anopheles stephensi*. *PLoS ONE* **2014**, *9*, e95988. [[CrossRef](#)] [[PubMed](#)]
88. Martin, E.; Bongiorno, G.; Giovati, L.; Montagna, M.; Crotti, E.; Damiani, C.; Gradoni, L.; Polonelli, L.; Ricci, I.; Favia, G.; et al. Isolation of a *Wickerhamomyces anomalus* yeast strain from the sandfly *Phlebotomus perniciosus*, displaying the killer phenotype. *Med. Vet. Entomol.* **2016**, *30*, 101–106. [[CrossRef](#)] [[PubMed](#)]